



# A Hermite CVBEM model of two-dimensional, steady-state, soil-water phase change

T.V. Hromadka II

Williamson & Schmid, 15101 Redhill Drive, Tustin, California 92680, USA and Department of Applied Mathematics, California State University, Fullerton, California 92634, USA

A linear trial function CVBEM model of a steady-state, two-dimensional freezing front is extended to the Hermite cubic polynomial trial function. The utility of this extension is demonstrated by the reduction in effort needed (over the linear trial function model) to develop an approximate boundary for error analysis, due to the derivative terms being included in the Hermite model. The modeling approach can be used not only for simple field problems, but also for the calibration of more sophisticated soil-water phase change models based on the more popular finite element and finite difference techniques.

## I BOUNDARY INTEGRAL APPROXIMATION EQUATION FORMULATION (CVBEM)

Because a thorough literature review and mathematical development of the CVBEM is contained in the book by Hromadka,<sup>8</sup> only the key equations needed to formulate each of the nodal point equations are provided in this paper. Additionally, discussions as to the usability of the CVBEM in engineering analysis, and also the convenient error analysis techniques provided by the CVBEM, are also found in the above reference.

Nodal point equations are developed in the following for the Principal Value of the Cauchy Integral for the Hermite cubic polynomial trial function. Because of the lengthy derivation, only the final equation forms (which would be used in a computer program) are presented. Detailed derivations involved in the linear trial function CVBEM model can be found in Hromadka,<sup>8</sup> and each of the higher order trial function derivations follow similar mathematical steps in their respective derivations of the nodal point equations.

Consider a simple connected domain,  $\Omega$ , with a simple closed contour boundary,  $\Gamma$ , as shown in Fig. 1. The boundary can be subdivided into  $m$  boundary elements,  $\Gamma_j$ , such that

$$\Gamma = \bigcup_{j=1}^m \Gamma_j \tag{1}$$

On each boundary element, define two nodal points located at the element end points; for element  $j$ , the

co-ordinates of the nodes are  $z_{j+1}$ . A Hermite cubic polynomial trial function,  $\alpha(s)$ , is assumed on each element such that

$$\alpha(s) = \bar{\omega}_j N_1(s) + \omega'_j N_2(s) + \omega_{j+1} N_3(s) + \omega'_{j+1} N_4(s); 0 \leq s \leq 1 \tag{2}$$

where  $\bar{\omega}_j$  is the complex nodal values for node  $j$ , and where  $\bar{\omega}_j = \bar{\phi}_j + i\bar{\psi}_j$ ; and  $\bar{\omega}'_j$  is the derivative of the complex variable function of node  $j$ . In eqn (2),  $\bar{\phi}_j$  and  $\bar{\omega}_j$  are state variable and stream function nodal values at co-ordinate  $z_j$ . The bar notation signifies a specified nodal value.

The CVBEM utilizes an integral function  $\hat{\omega}(z)$  defined by

$$2\pi i \hat{\omega}(z) = \sum_{j=1}^m \int_{\Gamma_j} \left( \frac{\alpha(\zeta) d\zeta}{\zeta - z} \right), z \in \Omega, z \notin \Gamma \tag{3}$$

where  $\zeta$  is the complex variable of integration,  $\alpha(\zeta)$  are the continuous trial functions, and subscript  $j$  refers to element contour  $\Gamma_j$ . Because the  $\alpha(\zeta)$  are continuous on  $\Gamma_j$ , the approximation function  $\hat{\omega}(z)$  is analytic for all  $z$  interior of  $\Gamma$ .

A boundary integral equation can be formulated for each nodal point by

$$2\pi i \hat{\omega}(z_1) = \lim_{z \rightarrow z_1} \sum_{j=1}^m \int_{\Gamma_j} \left( \frac{\alpha(\zeta) d\zeta}{\zeta - z} \right) \tag{4}$$

where the limit is evaluated as  $z$  approaches arbitrary nodal co-ordinate  $z_1$  from the interior of  $\Gamma$ . Solving eqn (4) results in the computation of the complex variable

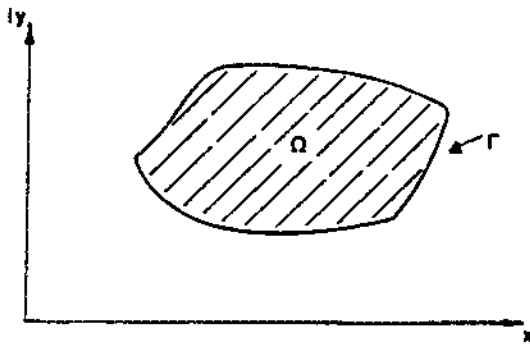


Fig. 1. Problem domain,  $\Omega$ , with boundary,  $\Gamma$ .

components,  $H_j$ , where

$$H_j = \ln \left( \frac{z_{j+1} - z}{z_j - z} \right) \quad (5)$$

Equation (5) is solved by noting

$$H_j = \ln \left( \frac{d(j+1, 1)}{d(j, 1)} \right) + i\theta(j+1, j) \quad (6)$$

and

$$H_1 = \ln \left( \frac{d(2, 1)}{d(m, 1)} \right) + i\theta(2, m)$$

In eqn (6),  $d(j+1, 1)$  is the distance between nodal co-ordinates  $z_{j+1}$  and  $z_1$ , and  $\theta(j+1, j)$  is the angle between co-ordinates  $z_{j+1}$  and  $z_j$  (Fig. 2).

An examination of the approximation function definition of eqn (3) reveals that  $\hat{\omega}(z)$  is a function of the boundary geometry and nodal values,  $\{\bar{\omega}_j, \bar{\omega}'_j\}$ . Should the assumed, trial functions  $\alpha(\zeta)$  be the solution of the boundary value problem, then  $\hat{\omega}(z)$  is the solution of the boundary value problem and  $\hat{\omega}(z) = \bar{\omega}(z)$ ,  $j = 1, 2, \dots, m$ . Generally, however,  $\hat{\omega}(z)$  is not the desired solution of  $\omega(z) = \phi + i\psi$ , and  $\hat{\omega}(z) \neq \bar{\omega}(z)$ .

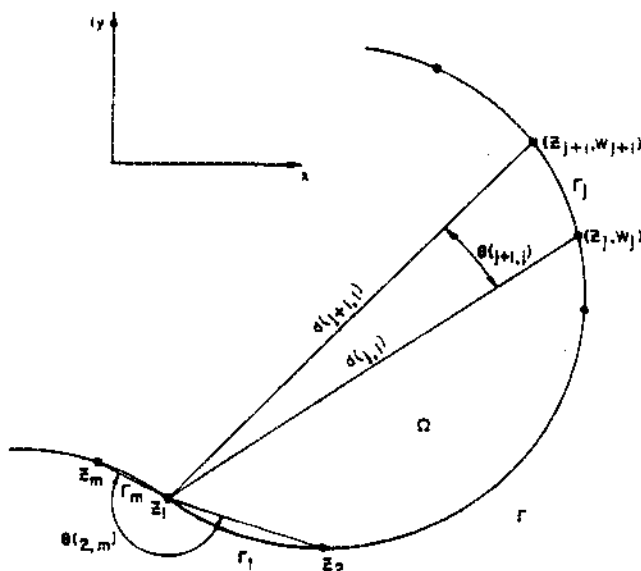


Fig. 2. CVBEM linear trial function geometry.

### CVBEM MODEL DEVELOPMENT

The CVBEM formulation results in a matrix system which, of course depends on the trial function definition. The nodal values,  $\bar{\omega}_j$ , are composed of two sets of components  $\bar{\omega}_j = \bar{\phi}_j + i\bar{\psi}_j$ ,  $\bar{\omega}'_j = \bar{\phi}'_j + i\bar{\psi}'_j$ , where one of either set of unknowns is specified at each  $z_j$  by the given boundary condition definitions. Consequently, each nodal point has two assigned known boundary values and two corresponding unknown boundary values. Should all four boundary nodal values be known at each  $z_j$ , then the approximation function  $\hat{\omega}(z)$  is defined throughout the interior of  $\Gamma$ . Therefore, in order to calculate  $\hat{\omega}(z)$  values, estimates of the unknown nodal boundary condition values are required. In the following discussion, it is assumed that  $\bar{\phi}_j$  and  $\bar{\phi}'_j$  are specified at each  $z_j$ , and the  $\bar{\psi}_j, \bar{\psi}'_j$  are unknown (except for a single nodal point value where the constant of integration is evaluated). The discussion is immediately extendable to the case of mixed boundary conditions. The following notation is used for the three sets of nodal point values:

$\omega_j = \omega(z_j) = \phi_j + i\psi_j$ ; exact solution of boundary value problem solution at node  $j$

$\bar{\omega}_j = \bar{\phi}_j + i\bar{\psi}_j$ ; boundary condition nodal values

$\hat{\omega}_j = \hat{\phi}_j + i\hat{\psi}_j$ ; approximation values at node  $j$

Solution of eqn (4) for each nodal point results in  $2m$  linear equations which can be written in matrix form as

$$\hat{\omega} = C_R(\bar{\phi}, \bar{\phi}', \bar{\psi}, \bar{\psi}') + iC_I(\bar{\phi}, \bar{\phi}', \bar{\psi}, \bar{\psi}') \quad (7)$$

where  $C_R$  and  $C_I$  are  $2m \times 4m$  matrices of real constants representing the real and imaginary parts of the boundary integral equations, respectively.

Since the values of the analytic functions  $\omega(z)$ , and its derivatives  $\omega'(z)$  are utilized at the nodal points, and we desire a cubic approximation, then define a continuous trial function of  $\Gamma_j$  by:

$$\alpha(\zeta) = \sum_{j=1}^n P_j(\zeta) \quad (8)$$

$$\alpha'(\zeta) = \sum_{j=1}^n P'_j(\zeta) \quad (9)$$

Where  $\alpha(\zeta)$  is defined as

$$\alpha(\zeta) = a_j - b_j\zeta + c_j\zeta^2 + d_j\zeta^3 \quad (10)$$

And the derivative  $\alpha'(\zeta)$  is given by:

$$\alpha'(\zeta) = b_j + 2c_j\zeta + 3d_j\zeta^2 \quad (11)$$

Collocating at the nodal points, we have four equations in four unknowns, which we solve to obtain the coefficients. Upon rearranging the coefficients, we get new expressions for  $\alpha(z)$  and  $\alpha'(z)$  at point  $z$ :

$$\alpha(z) = \bar{\omega}_j(Z_{2j})^2(1 + 2Z_{1j}) + \bar{\omega}_{j+1}(Z_{1j})^2(1 + 2Z_{2j}) + \bar{\omega}'_j Z_{1j} Z_{2j}(z_j - z) + \bar{\omega}'_{j+1} Z_{1j} Z_{2j}(z_j - z) \quad (12)$$

$$\begin{aligned} \alpha'(z) = & \bar{\omega}_j Z_{1j} Z_{2j} (6/(z_j - z_{j+1})) \\ & + \bar{\omega}_{j+1} Z_{1j} Z_{2j} (6/(z_{j+1} - z_j)) \\ & + \bar{\omega}'_j Z_{2j} (1 - 3Z_{1j}) \\ & + \bar{\omega}'_{j+1} Z_{1j} (1 - 3Z_{2j}) \end{aligned} \quad (13)$$

Where  $Z_{1j}$  and  $Z_{2j}$  are defined as

$$\begin{aligned} Z_{1j} &= \frac{(z - z_j)}{(z_{j+1} - z_j)} \\ Z_{2j} &= \frac{(z_{j+1} - z)}{(z_{j+1} - z_j)} \end{aligned}$$

**Principal value calculations**

Since we desire the value of the approximation functions on the boundary  $\Gamma$  as well as the interior of  $\Omega$ , we must consider the following equations:

$$\hat{\omega}(z) \cong \frac{1}{2\pi i} \sum_{j=1}^n \lim_{z_0 \rightarrow z} \int_{\Gamma_j} \frac{P_j(\zeta)}{\zeta - z_0} d\zeta \quad (14)$$

$$\hat{\omega}'(z) \cong \frac{1}{2\pi i} \sum_{j=1}^n \lim_{z_0 \rightarrow z} \int_{\Gamma_j} \frac{P_j(\zeta)}{\zeta - z_0} d\zeta \quad (15)$$

Simplifying the last integrals:

$$\begin{aligned} \hat{\omega}(z) \cong & \frac{1}{2\pi i} \lim_{z_0 \rightarrow z} \sum_{j=1}^n P_j(z) \ln \frac{(z_{j+1} - z_0)}{(z_j - z_0)} \\ & + \frac{1}{2\pi i} 2 \sum_{j=1}^n (\bar{\omega}_{j+1} - \bar{\omega}_j) Z_{1j} Z_{2j} \\ & + \frac{1}{2\pi i} \frac{1}{3} \sum_{j=1}^n \frac{(\bar{\omega}'_{j+1} + \bar{\omega}'_j)}{(z_{j+1} - z_j)} ((z_{j+1})^2 + z_{j+1} z_j) \\ & + \frac{1}{2\pi i} \frac{1}{3} \sum_{j=1}^n \frac{(\bar{\omega}'_{j+1} + \bar{\omega}'_j)}{(z_{j+1} - z_j)} (z_j^2 - 3z_{j+1} z_j) \\ & + \frac{1}{2\pi i} \frac{1}{3} \sum_{j=1}^n \frac{(\bar{\omega}'_{j+1} + \bar{\omega}'_j)}{(z_{j+1} - z_j)} (3z^2 - 3z_j z) \end{aligned} \quad (16)$$

$$\begin{aligned} \hat{\omega}'(z) \cong & \frac{1}{2\pi i} \lim_{z_0 \rightarrow z} \sum_{j=1}^n P_j'(z) \ln \frac{(z_{j+1} - z_0)}{(z_j - z_0)} \\ & + \frac{1}{2\pi i} 3 \sum_{j=1}^n \frac{(z_{j+1} - z_j - 2z)}{(z_{j+1} - z_j)} \frac{(\bar{\omega}_{j+1} - \bar{\omega}_j)}{(z_{j+1} - z_j)} \\ & - \frac{1}{2\pi i} 3 \sum_{j=1}^n \frac{(z_{j+1} - z_j - 2z)}{(z_{j+1} - z_j)} \frac{(\bar{\omega}'_{j+1})}{2} \\ & - \frac{1}{2\pi i} 3 \sum_{j=1}^n \frac{(z_{j+1} - z_j - 2z)}{(z_{j+1} - z_j)} \frac{(\bar{\omega}'_j)}{2} \end{aligned} \quad (17)$$

Which are valid for  $z \in \Omega$ .

The terms involving logarithms in (16) and (17) are simplified as

$$\begin{aligned} \lim_{z_0 \rightarrow z_k} \sum_{j=1}^n P_j(z_k) \ln \frac{(z_{j+1} - z_0)}{(z_j - z_0)} \\ = \sum_{j=1, \neq k, k-1}^n P_j(z_k) \ln \frac{(z_{j+1} - z_k)}{(z_j - z_k)} \end{aligned}$$

$$\begin{aligned} & + \bar{\omega}_k \ln \frac{(z_{k+1} - z_k)}{(z_{k-1} - z_k)} \\ \lim_{z_0 \rightarrow z_k} \sum_{j=1}^n P_j'(z_k) \ln \frac{(z_{j+1} - z_0)}{(z_j - z_0)} \\ = \sum_{j=1, \neq k, k-1}^n P_j'(z_k) \ln \frac{(z_{j+1} - z_k)}{(z_j - z_k)} \\ & + \bar{\omega}'_k \ln \frac{(z_{k+1} - z_k)}{(z_{k-1} - z_k)} \end{aligned} \quad (19)$$

Where  $z_k$  is a nodal point of  $\Gamma$  and  $z_0 = z_k, z_{k-1} = z_1$ .

**Matrix development**

To implement the Hermite CVBEM, the equations from the above development are simplified to obtain the following:

$$\begin{aligned} \bar{\omega}_k \cong & \frac{1}{2\pi i} \sum_{j=1}^n (\bar{\omega}_{j+1} cc1jk - \bar{\omega}_j cc1jk) \\ & + \frac{1}{2\pi i} \sum_{j=1}^n (\bar{\omega}'_{j+1} cc2jk + \bar{\omega}'_j cc2jk) \\ & + \frac{1}{2\pi i} \sum_{j=1, \neq k, k-1}^n (\bar{\omega}_{j+1} cc6jk + \bar{\omega}_j cc5jk) \\ & + \frac{1}{2\pi i} \sum_{j=1, \neq k, k-1}^n (\bar{\omega}'_{j+1} cc8jk + \bar{\omega}'_j cc7jk) \\ & + \frac{1}{2\pi i} \bar{\omega}_k \ln \frac{(z_{k+1} - z_k)}{(z_{k-1} - z_k)} \end{aligned} \quad (20)$$

Where  $cc1jk, cc2jk, cc5jk, cc6jk, cc7jk,$  and  $cc8jk$  are functions of the geometry of the nodal points.

Let  $\bar{\omega}_1 = \phi_1 + i\psi_1$  and define  $c1, c2, c3,$  and  $c4$  as a function of nodal orientation, i.e.:

If  $j \neq k, k - 1$ , then:

$$\begin{aligned} c1jk &= cc1jk + cc6jk \\ c2jk &= cc1jk + cc5jk \\ c3jk &= cc2jk + cc8jk \\ c4jk &= cc2jk + cc7jk \end{aligned} \quad (21)$$

If  $j = k$  or  $j = k - 1$ , then:

$$\begin{aligned} c1jk &= cc1jk \\ c2jk &= -cc1jk \\ c3jk &= cc2jk \\ c4jk &= cc2jk \end{aligned}$$

If we now expand eqn (20) and separate real and imaginary components we obtain:

$$\begin{aligned} \phi_k \cong & \frac{1}{2\pi} \sum_{j=1}^n [\phi_{j+1} \text{Im}(c1jk) + \psi_{j+1} \text{Re}(c1jk)] \\ & + \frac{1}{2\pi} \sum_{j=1}^n [\phi_j \text{Im}(c2jk) + \psi_j \text{Re}(c2jk)] \end{aligned}$$

$$\begin{aligned}
& + \frac{1}{2\pi} \sum_{j=1}^n [\phi'_{j+1} \operatorname{Im}(c3jk) + \psi'_{j+1} \operatorname{Re}(c3jk)] \\
& + \frac{1}{2\pi} \sum_{j=1}^n [\phi'_j \operatorname{Im}(c4jk) + \psi'_j \operatorname{Re}(c4jk)] \\
& + \frac{1}{2\pi} \phi_k \operatorname{Im} \left( \ln \frac{(z_{k+1} - z_k)}{(z_{k-1} - z_k)} \right) \\
& + \frac{1}{2\pi} \psi_k \operatorname{Re} \left( \ln \frac{(z_{k+1} - z_k)}{(z_{k-1} - z_k)} \right) \quad (22) \\
\psi_k \cong & \frac{1}{2\pi} \sum_{j=1}^n [\phi_{j+1} \operatorname{Re}(c1jk) - \psi_{j+1} \operatorname{Im}(c1jk)] \\
& - \frac{1}{2\pi} \sum_{j=1}^n [\phi_j \operatorname{Re}(c2jk) - \psi_j \operatorname{Im}(c2jk)] \\
& - \frac{1}{2\pi} \sum_{j=1}^n [\phi'_{j+1} \operatorname{Re}(c3jk) - \psi'_{j+1} \operatorname{Im}(c3jk)] \\
& - \frac{1}{2\pi} \sum_{j=1}^n [\phi'_j \operatorname{Re}(c4jk) - \psi'_j \operatorname{Im}(c4jk)] \\
& - \frac{1}{2\pi} \phi_k \operatorname{Re} \left( \ln \frac{(z_{k+1} - z_k)}{(z_{k-1} - z_k)} \right) \\
& + \frac{1}{2\pi} \psi_k \operatorname{Im} \left( \ln \frac{(z_{k+1} - z_k)}{(z_{k-1} - z_k)} \right) \quad (23)
\end{aligned}$$

Where  $\operatorname{Re}(c)$  and  $\operatorname{Im}(c)$  indicate the real and imaginary components of a complex constant  $c$ . An exactly analogous procedure can be performed to obtain a similar representation for  $\phi'_k$  and  $\psi'_k$ .

## II MODELING APPROACH FOR TWO-DIMENSIONAL, STEADY-STATE, SOIL-WATER PHASE CHANGE MODEL

The use of the Complex Variable Boundary Element Method to model soil-water phase change effects is a new numerical approach to this class of problems. In previous work, Hromadka & Guymon<sup>1</sup> applied the Complex Variable Boundary Element Method (CVBEM) to the problem of predicting freezing fronts in two-dimensional soil systems. Hromadka *et al.*<sup>2</sup> subsequently compare the CVBEM solution to a domain solution method and prototype data for the Deadhorse Airport runway at Prudhoe Bay, Alaska. In another work, the model is further extended to include an approximation of soil-water flow.<sup>3</sup> In contrast to the CVBEM approach, an example in the use of real variable boundary element methods in the approximation of such moving boundary phase change problems and a review of the pertinent literature is given in O'Neill.<sup>10</sup>

Hromadka & Guymon<sup>4</sup> develop a relative error estimation scheme which exactly evaluates the relative error distribution on the problem boundary that results from the CVBEM approximator matching the known boundary conditions. This relative error determination is

used to add or delete boundary nodes to improve accuracy. Thus, the CVBEM permits a direct and immediate determination of the approximation error involved in solution of an assumed Laplacian system. The modeling accuracy is evaluated by the model-user in the determination of an approximate boundary upon which the CVBEM provides an exact solution. Although inhomogeneity (and anisotropy) can be included in the CVBEM model, the resulting fully-populated matrix system quickly becomes large. Therefore in this work, the domain is assumed homogeneous and isotropic except for differences in frozen and thawed conduction parameters for freezing and thawing problems, respectively. Hromadka<sup>9</sup> developed a linear trial function model; in this paper, the cited work is extended to the case of using a Hermite cubic polynomial trial function. Because of the direct analogy between the Hermite CVBEM model and the model in Hromadka,<sup>9</sup> the reader is referred to that citation for model details.

A major benefit in the use of the CVBEM over other numerical methods (including real variable boundary element methods and domain methods such as finite-differences and finite-elements) is the accurate and easy-to-use 'approximation boundary' error evaluation technique. Often, the CVBEM approximation analysis is terminated when the approximate boundary differs from the true problem boundary to within the construction tolerance of the project, resulting in an exact CVBEM model of a probable constructed version of the engineered plan drawings. Consequently, the CVBEM approach can be used directly in engineering applications, or used to provide a wide range of highly accurate approximations for two-dimensional phase change problems (where the freezing front movement is slow) for checking modeling results produced by other numerical methods.

## HEAT FLOW MODEL

For a wide range of soil freezing (or thawing) problems, the freezing front movement is sufficiently slow such that the governing heat flow equation can be modeled using a timestepped steady heat flow approximation. That is for small durations of time, the heat flux along the freezing front can be computed assuming the temperature distribution within the frozen (or thawed) regions are potential functions (i.e. the Laplace equation applies). Figure 3 illustrates a typical two-phase problem definition where the heat flow model solves for heat flux along the freezing front by solving the Laplace equation (by use of potential functions) in both the frozen and thawed regions.

To develop mathematical models of the Laplace equation in each region, a CVBEM approximator is generated which matches specified boundary conditions of either temperature or flux at nodal point locations on the problem boundary and freezing front. The CVBEM approximator exactly satisfies the Laplace equation;

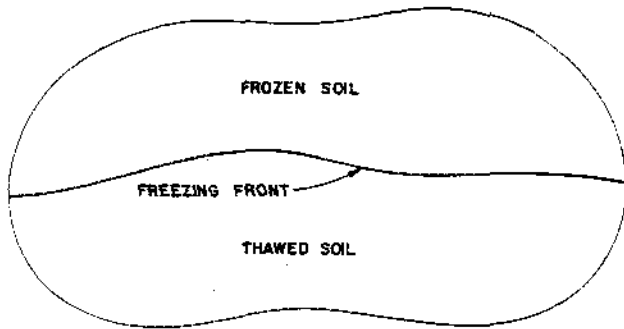


Fig. 3. Typical two-phase problem definition.

consequently there is no modeling error in solving the governing Laplace equation (heat flow model), there is only error in matching the boundary conditions continuously. Figure 4 shows an example roadway problem where the freezing front is initially located some known distance below the surface. Boundary conditions for the example problem and a nodal point placement scheme are shown in Fig. 5.

### PHASE CHANGE MODEL

For each timestep, a CVBEM approximation function is developed for both the frozen and thawed portions of the problem domain based on the problem geometry and boundary conditions. Heat flux is computed along the freezing front using the CVBEM approximation function derivative values. The heat flux estimates are assumed to directly equate to the rate of freezing (or thawing) of a volume of soil at the freezing front. For the example of Fig. 5, freezing results in a downward migration of the freezing front such that the product of the timestep and heat flux equals the latent heat evolved by the change in freezing front coordinates.

Two freezing front displacement models are available:

- (1) All displacement occurs in the vertical direction. This simplified model is generally appropriate for many roadway problems.
- (2) Displacement computed based on an outward normal vector. This model may be the most

accurate, but requires additional computational effort than the vertical displacement model. Figure 6 shows the nodal point displacement in a direction which balances the angles to go between the normal vector and boundary elements.

### Class of problems modeled

The CVBEM model may be used to study soil-water freezing (or thawing) in two-dimensional, homogeneous, isotropic domains. The current version of the Hermite CVBEM model accommodates only one region (i.e. either entirely frozen or entirely thawed) and the freezing front forms part of the control volume's boundary. Thus, the model may be used to study the freezing front advancement into a soil system where the soil system is initially close to the freezing point depression temperature, and negligible heat flow to the freezing front is contributed from the underlying soil system. A schematic of the problem domain and boundary conditions are illustrated in Fig. 7. Another characteristic of the current Hermite CVBEM model is that the boundary conditions of the problem are held constant for the entire simulation. Additionally, the initial conditions of the problem are assumed to be near steady-state with the freezing front specified some distance below the top of the control volume boundary (control surface). The modeling procedure used is shown schematically in Fig. 8 for the case of a soil freezing problem.

### III MODELING ERROR ANALYSIS

A major benefit afforded by the CVBEM is the available error analysis. Because the approximation function,  $\hat{\omega}(z)$ , is an analytic function, then its real and imaginary components ( $\hat{\phi}(z)$  and  $\hat{\psi}(z)$ ) both exactly satisfy the Laplace equation. However, the  $\hat{\omega}(z)$  does not generally satisfy the boundary conditions of the problem.

However, an approximate boundary,  $\hat{\Gamma}$ , can be developed where  $\hat{\omega}(z)$  satisfies the boundary conditions.  $\hat{\Gamma}$  is developed by locating where in space,  $\hat{\omega}(z)$  equals the

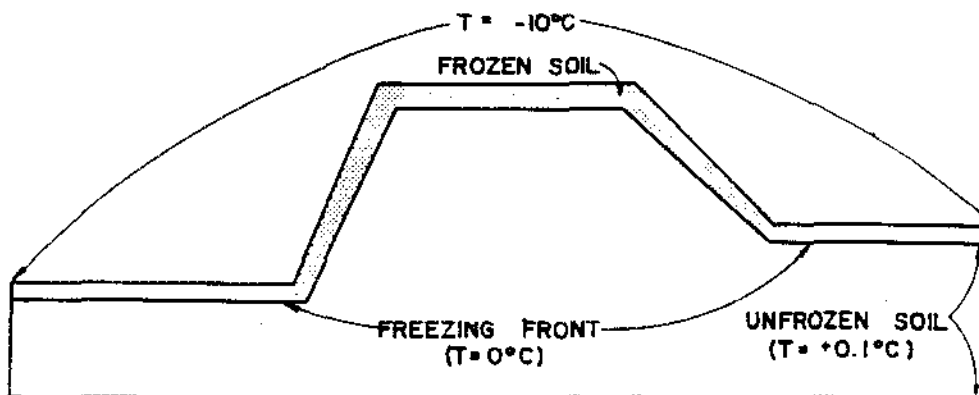


Fig. 4. Typical roadway embankment problem.

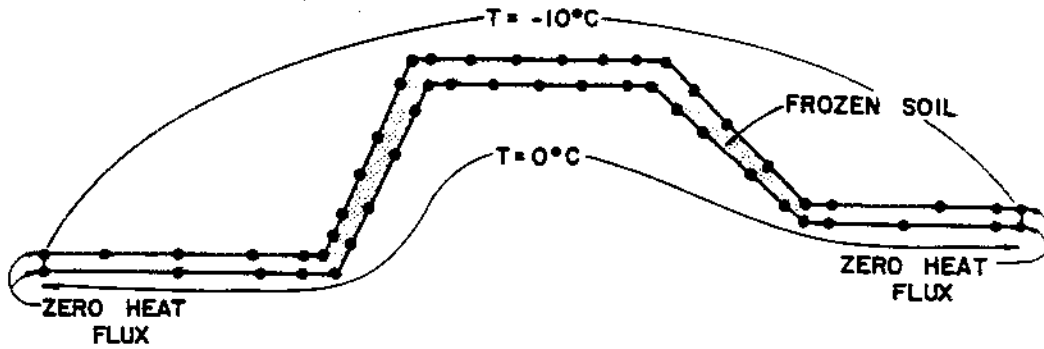


Fig. 5. Nodal point placement and boundary conditions for the Fig. 4 problem.

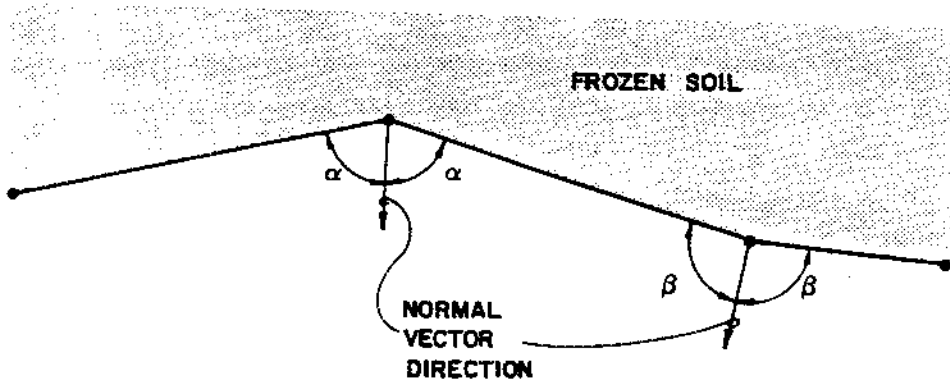


Fig. 6. Normal vector coordinate displacement model (note balanced angles for each normal vector).

boundary conditions (e.g. where  $\hat{\phi}(z) = 0^\circ\text{C}$  at the freezing front).

For example, along the freezing front  $\phi(z) = 0^\circ\text{C}$ . However,  $\hat{\phi}(z) \neq 0^\circ\text{C}$  except at scattered locations along the boundary elements. If  $\hat{\phi}(z) = +0.1^\circ\text{C}$ , at some location, the  $0^\circ\text{C}$  isotherm is located by utilizing the Cauchy-Riemann equations (see Hromadka,<sup>8</sup> and Fig. 9). The Hermite polynomial directly computes the derivatives  $\partial\phi/\partial n$  and  $\partial\psi/\partial s$ . The component  $\partial\psi/\partial s$  is used to evaluate the displacement between  $\Gamma$  and  $\hat{\Gamma}$  at any point

$z$  on  $\Gamma$  by dividing the difference  $(\phi(z) - \hat{\phi}(z))$  by  $\partial\psi/\partial s$  (see Hromadka<sup>9</sup>).

#### IV CONCLUSIONS

A linear trial function CVBEM model of a steady-state, two-dimensional freezing front is extended to the Hermite cubic polynomial trial function. The utility of

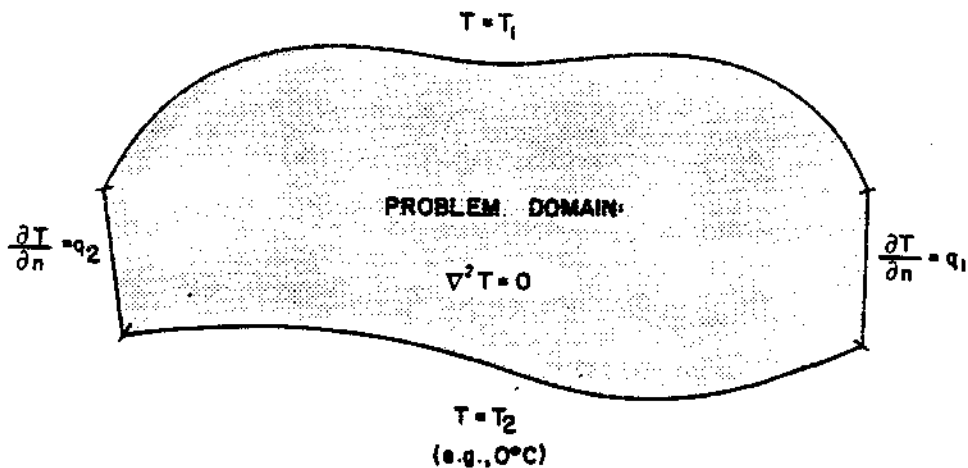
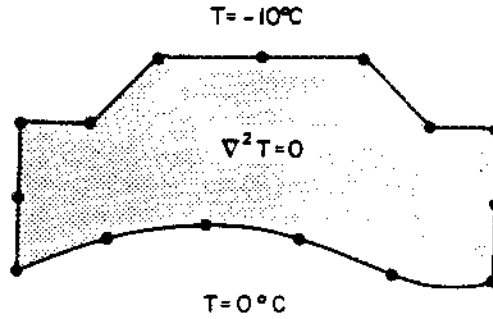
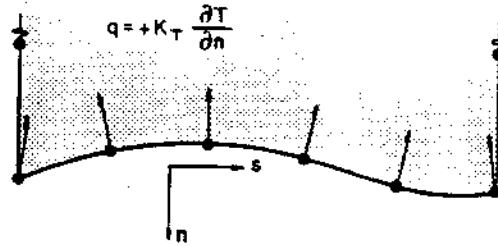


Fig. 7. Program boundary condition characteristics.

DEVELOP A CVBEM APPROXIMATOR BASED ON BOUNDARY COORDINATES AND BOUNDARY CONDITIONS



CALCULATE HEAT FLUX VALUES ALONG THE FREEZING FRONT



DISPLACE NODAL COORDINATES ALONG FREEZING FRONT BASED ON HEAT EVOLVED, AND VOLUMETRIC LATENT HEAT OF FUSION FOR SOIL-WATER MIXTURE

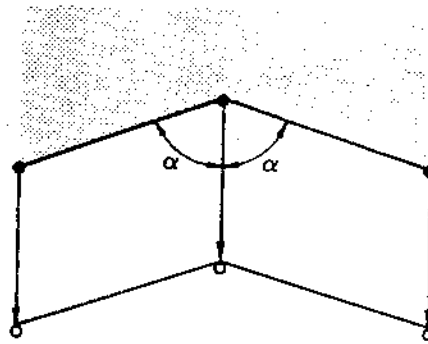


Fig. 8. Freezing front evolution modeling procedure.

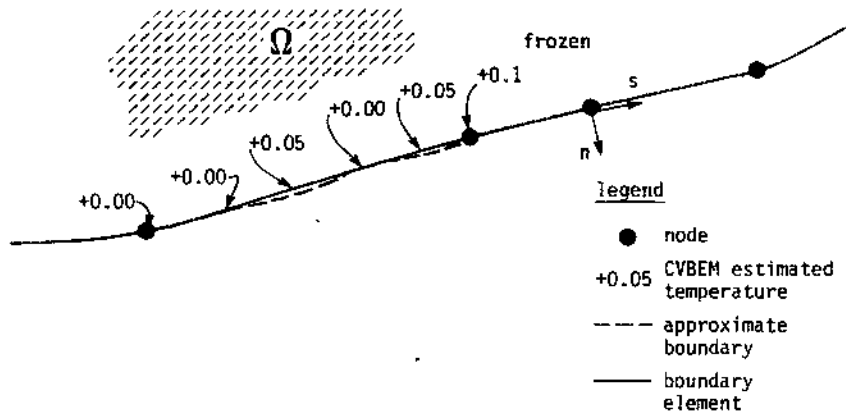


Fig. 9. Locating the 0°C isotherm.

this extension is demonstrated by the reduction in effort needed (over the linear trial function mode) to develop an approximate boundary for error analysis, due to the derivative terms being included in the Hermite model. The modeling approach can be used not only for simple field problems, but also for the calibration of more sophisticated soil-water phase change models based on the more popular finite element and finite difference techniques.

Future research needed is the inclusion of inhomogeneity and variable boundary conditions. An unavoidable aspect of the CVBEM technique is the inability to extend to three-dimensions; however, many problems are two-dimensional and the provided approach provides an advantage due to the unique error evaluation.

Possibly, the greatest utility of this model is the generation of quasi-analytic solutions to two-dimensional steady-state soil-water phase change problems which can be used to verify other numerical models.

## REFERENCES

1. Hromadka II, T.V. & Guymon, G.L. Application of a boundary integral equation to prediction of freezing fronts in soils, *Cold Regions Science & Technology*, 1982, (6), 115-121.
2. Hromadka II, T.V., Guymon, G.L. & Berg, R.L. Comparison of two-dimensional domain and boundary integral geothermal models with embankment freeze-thaw field data, *Fourth Int. Permafrost Conference*, Fairbanks, Alaska, 1983.
3. Hromadka II, T.V. & Guymon, G.L. A simple model of ice segregation using an analytic function to model heat and soil-water flow, *ASME Third International Symposium on Offshore Mechanics and Arctic Engineering*, New Orleans, LA, 1984.
4. Hromadka II, T.V. & Guymon, G.L. An algorithm to reduce approximation error from the Complex Variable Boundary Element Method applied to soil freezing, *Numerical Heat Transfer*, 1985, 8(1), 115-130.
5. Hromadka II, T.V. & Guymon, G.L. A Complex Variable Boundary Element Method: Development, *International Journal of Numerical Methods in Engineering*, 1984.
6. Hromadka II, T.V. *The Complex Variable Boundary Element Method* Springer-Verlag Publishers, 1984.
7. Hromadka II, T.V. & Durbin, T.J. Adjusting the nodal point distribution in domain groundwater flow numerical models, *Proceedings, Fifth International Conference on FEM in Water Resources*, University of Vermont, 1984.
8. Hromadka II, T.V. & Lai, C. *The Complex Variable Boundary Element Method in Engineering Analysis*, Springer-Verlag Publishers, 1987.
9. Hromadka II, T.V. Tracking two-dimensional freezing front movement using the Complex Variable Boundary Element Method, U.S. Army Corps of Engineers, Cold Regions Research & Engineering Laboratory, Special Report 87-8, 1987.
10. O'Neill, K. Boundary Integral Equation solution of moving boundary phase change problems, *Int. J. Num. Mech. Engg.*, 1983, 19, 1825-1850.
11. Outcalt, S. A simple energy balance model of ice segregation, *Cold Regions Science and Technology*, 1980, 3, 145-151.
12. Yoo, J. & Rubinsky, B. Numerical computation using finite elements for the moving interface in heat transfer problems with phase transformation, *Numerical Heat Transfer*, 1983, 6.